SPONTANEOUS MUTANTS OF *STREPTOCOCCUS SANGUINIS* WITH DEFECTS IN THE GLUCOSE-PTS SHOW ENHANCED POST-EXPONENTIAL PHASE FITNESS

Lin Zeng[#], Alejandro R. Walker, Kyulim Lee*, Zachary A. Taylor, and Robert A. Burne

Department of Oral Biology, University of Florida College of Dentistry, 1395 Center Drive, Gainesville, Florida, USA.

Running title: Glucose-PTS regulates bacterial persistence

[#] Correspondence

Lin Zeng, PhD

lzeng@dental.ufl.edu

* Present address: Nationwide Children's Hospital, Columbus, Ohio, USA.

Keywords: Carbohydrate metabolism, glucose-PTS, *Streptococcus sanguinis*, pyruvate metabolism, single-nucleotide polymorphism, bacterial persistence.

Abstract

Genetic truncations in a gene encoding a putative glucose-PTS protein (*manL*, $EIIAB^{Man}$) were identified in subpopulations of two separate laboratory stocks of *Streptococcus sanguinis* SK36; the mutants had reduced PTS activities on glucose and other monosaccharides. Using an engineered mutant of *manL* and its complemented derivative, we showed that the ManL-deficient strain had improved bacterial viability in stationary phase and was better able to inhibit the growth of the dental caries pathogen *Streptococcus mutans*. Transcriptional analysis and biochemical assays suggested that the *manL* mutant underwent reprograming of central carbon metabolism that directed pyruvate away from production of lactate, increasing production of hydrogen peroxide (H_2O_2) and excretion of pyruvate. Addition of pyruvate to the medium enhanced the survival of SK36 in overnight cultures. Meanwhile, elevated pyruvate levels were detected in the cultures of a small, but significant percentage (~10%), of clinical isolates of oral commensal bacteria. Furthermore, the *manL* mutant showed higher expression of the arginine deiminase system than the wild type, which enhanced the ability of the mutant to raise environmental pH when arginine was present. Significant discrepancies in genome sequence were identified between strain SK36 obtained from ATCC and the sequence deposited in GenBank. As the conditions that are likely associated with the emergence of spontaneous *manL* mutations, i.e. excess carbohydrates and low pH, are those associated with caries development, we propose that the glucose-PTS strongly influences

commensal-pathogen interactions by altering the production of ammonia, pyruvate, and H_2O_2.

Importance A health-associated dental microbiome provides a potent defense against pathogens and diseases. *Streptococcus sanguinis* is an abundant member of a health-associated oral flora that antagonizes pathogens by producing hydrogen peroxide. There is a need for a better understanding of the mechanisms that allow bacteria to survive carbohydrate-rich and acidic environments associated with the development of dental caries. We report the isolation and characterization of spontaneous mutants of *S. sanguinis* with impairment in glucose transport. The resultant reprograming of central metabolism in these mutants reduced the production of lactic acid and increased pyruvate accumulation; the latter enables these bacteria to better cope with hydrogen peroxide and low pH. The implications of these discoveries in the development of dental caries are discussed.

Introduction

Dental caries is caused by dysbiosis in the dental microbiome, where an overabundance of acid-producing (acidogenic) and acid-resistant (aciduric) bacteria such as mutans streptococci and lactobacilli, along with certain *Actinomyces, Scardovia*, and fungal species, drives the acidification of dental biofilms and demineralization of tooth enamel. Diets rich in carbohydrates are critical to caries formation, while host genetics and socioeconomic factors also

affect the incidence and severity of the disease(s) (1, 2). Organic acids, including lactic, acetic, and formic, are some of the primary products released by oral bacteria that ferment carbohydrates, which include bacteria that are considered etiological agents of caries and those that are considered commensals. Due to its low p*Ka* value, lactic acid is particularly damaging to tooth enamel. When dietary carbohydrates are ingested, lactate can be produced in large quantities by a group of oral streptococci that includes *Streptococcus mutans*, the primary etiological agent of dental caries. Other bacterial factors important to the ecological balance of the dental microbiome include reactive oxygen species, e.g. hydrogen peroxide (H_2O_2) and alkaline compounds, such as ammonia. Many bacteria, *S. mutans* in particular, are sensitive to physiologically relevant concentrations of H_2O_2, and thus can be inhibited by the presence of peroxigenic commensals, mainly mitis group of streptococci, which includes *S. sanguinis, Streptococcus gordonii, Streptococcus mitis* and other commensal streptococci that are among the most abundant members of the dental microbiome (3). Generally, *S. sanguinis* and *S. gordonii* are considerably less acid tolerant (aciduric) than *S. mutans*, but carry the arginine deiminase (AD) system, which in the presence of arginine, releases ammonia and provides ATP to improve the survival and persistence of these organisms when faced with an acid challenge (4). Past research has indicated that production of both H_2O_2 (5-7) and AD activities (8) by these commensals can be influenced by bacterial uptake and catabolism of specific carbohydrates.

For most oral streptococci, carbohydrates are primarily internalized via the phosphoenolpyruvate::sugar phosphotransferase system (PTS), which is composed of two general proteins, Enzyme I (EI) and the phospho-carrier protein HPr, and a variety of carbohydrate-specific Enzymes II (EII) that are membrane-associated permeases (9). The PTS concurrently internalizes and phosphorylates carbohydrates that can be fed into the Embden-Meyerhoff-Parnas (EMP) pathway, which primarily yields pyruvate and the energy molecules ATP and NADH. To maintain bacterial redox balance and resupply glycolysis, NADH must be oxidized back into NAD^+. In oral streptococci, this can occur via lactate dehydrogenase (LDH) (10), an NADH oxidase (NOX), or other redox-coupled reactions (11). As the central point for bacterial energy metabolism and biogenesis, pyruvate can supply the tricarboxylic acid cycle (TCA) for bacteria that can conduct aerobic respiration, or alternatively can be converted to the aforementioned organic acids when oxygen is limited. As most of the streptococci have only a partial TCA cycle and lack cytochromes, the fate of pyruvate is limited to either homolactic fermentation, yielding lactic acid via the reducing activity of LDH, or heterofermentation that can produce ethanol, acetic acid, formate, and other end products depending on conditions and carbohydrate source(s)(12, 13). Oxidation of pyruvate by a few non-LDH pathways, including pyruvate dehydrogenase (PDH), pyruvate-formate lyase (Pfl), and pyruvate oxidase (POX) allows the bacteria to create more energy molecules and produce end products with either milder or no acidic properties. It is primarily the activity of POX, encoded by *spxB* in *S. sanguinis*, that produces H_2O_2; *S. mutans* lacks

spxB and does not produce H_2O_2 in any significant quantities. Distribution of pyruvate between the LDH and non-LDH pathways is regulated at both the transcriptional and enzymatic levels in response to bacterial energy status, generally metabolic intermediates such as fructose-1,6-bisphosphate (F-1,6-bP), and environmental cues such as carbohydrate abundance, pH, and oxygen levels (10, 12). The LDH pathway is usually favored under low-oxygen and carbohydrate-excess conditions.

As one of the early colonizers of oral cavity, *S. sanguinis* is an abundant commensal species that is frequently associated with oral health (14). It is also considered an opportunistic pathogen of infective endocarditis (IE). Previous research has indicated that *S. sanguinis* can ferment a large array of carbohydrates for acid production (15). *In silico* analyses also identified PTS transporters and metabolic pathways that are comparable to those in other more-intensively studied streptococcal species, such as *S. mutans* (16, 17). Notably different from *S. mutans*, *S. sanguinis* possesses the genes necessary to carry out gluconeogenesis, oxidation of pyruvate to produce H_2O_2, and the full functions of the pentose phosphate pathway. Recently, a transcriptomic study delineated in *S. sanguinis* SK36 the regulon governed by the transcriptional regulator CcpA (18), which in many Gram-positive Firmicutes is the dominant regulator of carbohydrate catabolite repression (CCR), a phenomenon where the genes encoding metabolic pathways for non-preferred carbohydrates are transcriptionally suppressed until a preferred carbohydrate such as glucose has been exhausted (19). Loss of CcpA in *S. sanguinis* SK36 affected expression of

nearly 20% of the genome. Interestingly, studies on the effects of *ccpA* deletion in *S. sanguinis* reported enhanced secretion of H_2O_2 without a significant change in antagonistic potential against *S. mutans*. Expression of *spxB* was shown to be regulated by CcpA, but the increased secretion by the *ccpA* mutant of pyruvate, an antioxidant, was postulated to counteract the impact of overproduction of H_2O_2 (20, 21).

We recently identified a memory effect of sugar metabolism in *S. mutans*, where past catabolism of monosaccharides, such as glucose and fructose, had profound impacts on the capacity of the bacterium to utilize lactose (22). To ascertain whether the memory effect was a general behavior of oral streptococci, these investigations were expanded to include *S. sanguinis* SK36, and a deletion mutant of the lactose repressor LacR was constructed to study its function in regulating catabolism of multiple carbohydrates. Here, we report the unexpected identification of spontaneous glucose-PTS mutations in two SK36 stocks that afforded a subpopulation of the cells enhanced fitness under laboratory conditions. Further analysis indicated that the PTS plays an important role in the regulation of central carbon metabolism in *S. sanguinis* in ways that contribute to the ability of this commensal to persist under stress and to compete against the pathobiont *S. mutans*.

Results

Isolation from SK36 of spontaneous mutants deficient in glucose PTS. We previously investigated the impact on carbohydrate metabolism of deletion of a

lactose repressor gene *lacR* in *S. sanguinis* SK36 (22). When analyzing growth and carbohydrate transport in the *lacR* mutant of SK36, we noted an unusually severe defect in PTS activity compared to similarly constructed *lacR* mutants we had created in related bacteria. In an effort to understand the basis of this phenotype, we conducted whole genome sequencing (WGS) of the *lacR* mutant and, as a control, the parental strain of frozen stock of SK36 (here designated as strain MMZ1612). Results of the WGS indicated the presence in our wild-type laboratory strain of SK36 (MMZ1612) of 115 single-nucleotide polymorphisms (SNPs, Table S1) that were not present in the published genome of SK36 available at GenBank. Notably, there were two truncations, one being a 330-bp deletion in a putative glucose-PTS gene (SSA_1918, tentatively identified as *manL*) that encodes the A and B domains of the Enzyme II of a PTS permease (23), and the other a 342-bp deletion in an open reading frame (ORF) (SSA_1927) that encodes for a putative transporter predicted to confer tellurite resistance (24). The SSA_1918 would have resulted in a translational product that terminates before the EIIB domain of the apparent ManL homologue. Two PCR reactions were designed based on this information and used to assess the integrity of the *manL* gene and SSA_1927 in random isolates selected from individual colonies grown from our MMZ1612 frozen stock. The results provided evidence that these two deletions were likely present in a subpopulation of the stock, comprising roughly 30% of the viable cells.

Subsequently, a second attempt was made at creating the *lacR* deletion, by requesting a different stock of SK36 (here designated MMZ1896) from the

177 laboratory of Todd Kitten, which works extensively with SK36. After performing
178 the same genetic manipulation, similar growth phenotypes (data not shown) were
179 noted in some of the *lacR*-null clones that again suggested a deficiency in
180 glucose-PTS activity. WGS, followed by PCR for selected regions of the genome,
181 indeed identified a nonsense mutation event, Q217* (CAA→TAA), in ~10% of the
182 population that resulted in truncation of the SSA_1918/*manL* gene at
183 approximately the same location as in MMZ1612. Similar to our SK36 stock
184 (MMZ1612), 114 SNPs were identified in MMZ1896 (Kitten stock; Table S1),
185 which, except for one, matched what was found in our freezer stock (MMZ1612).
186 The genetic lesions in *manL* could reduce the capacity of *S. sanguinis* to utilize a
187 number of carbohydrates commonly present in the human oral cavity, since the
188 ManLMN permease in *S. mutans* is the primary transporter for glucose,
189 galactose, glucosamine (GlcN) and N-acetylglucosamine (GlcNAc) (see Fig. S1
190 for growth curves). Indeed, when a wild-type copy of the *lacR* gene was later
191 introduced into one such *lacR*-null strain using an integration vector pMJB8 (25),
192 the complemented strain remained deficient in growth on glucose and certain
193 other monosaccharides dependent on the ManLMN glucose-PTS for
194 internalization (data not shown). Nonetheless, the fact that these mutants are so
195 well-represented in populations could indicate that there are physiological
196 benefits associated either with the specific lesions in the glucose-PTS or with
197 other not-yet-investigated SNPs that, under certain conditions, outweighed the
198 reduced fitness associated with loss of a primary hexose internalization system.
199

Enhanced persistence of *manL* mutants under acidic stress. To further investigate the involvement of the glucose-PTS in the observed behaviors, a number of *manL* deletion mutants were constructed in the backgrounds of wild-type isolates of SK36 (MMZ1612 and MMZ1896) via the allelic exchange method (Table 1). To rule out the possibility of additional spontaneous mutations obscuring the effects of *manL* deletion, two *manL*-complemented derivatives (*manLComp*) were constructed in the *manL*-null background via a “knock-in” approach (26). The wild-type parent SK36, a *manL* mutant and a *manLComp* strain were first studied for their growth phenotypes. Strains were cultivated to exponential phase in BHI before diluting into the chemically-defined medium FMC formulated with glucose, galactose, GlcN or GlcNAc as the sole carbohydrate source. Compared to the wild type and the complemented strain, *manL* mutant strains showed reduced growth rates on glucose and galactose, and especially poor growth on the amino sugars GlcN and GlcNAc (Fig. S2). The growth defects in the *manL* mutant were similar to those of the aforementioned *lacR* mutant (Fig. S1). To assess long term viability and effects of pH thereon, we streaked the strains on BHI agar or BHI agar supplemented with 50 mM potassium phosphate buffer (pH 7.2). Wild-type SK36 remained viable for at least 3 weeks at 4°C on the buffered plates, whereas viable cells could not be recovered from unbuffered plates after a week or less. Conversely, the *manL* mutant survived one to two weeks longer than SK36 on unbuffered BHI agar. When tested for growth characteristics by diluting directly from overnight cultures, deletion of *manL*, or addition of phosphate buffer in the overnight cultures,

223 significantly shortened the lag phase following sub-culture into fresh BHI or into
224 TY medium supplemented with glucose (TY-Glc) (Fig. 1AB). These effects
225 indicated improved viability in the overnight cultures as a result of *manL* deletion,
226 and that loss of viability likely involved exposure to lower pH values than in
227 buffered media. To further examine the relative fitness of the strains, overnight
228 cultures of SK36 and the *manL* mutant were used in a competition assay by
229 mixing in a 1:1 ratio (based on OD_{600}) and diluting 1000-fold into fresh BHI
230 medium. After one more round of dilution (at 5 h) followed by an overnight
231 incubation (24 h), cells were plated for CFU enumeration on selective agar
232 plates. Competition indices (CI) were calculated using CFUs at 0 and 24 h time
233 points. Out of the three replicates, *manL* outcompeted the wild-type parent by a
234 large margin in two biological replicates, with CI = 25.1 and 9.9; and in the third
235 replicate SK36 was no longer detected. These results strongly supported the
236 notion of enhanced fitness due to deletion of *manL*, providing a potential
237 explanation for the emergence of glucose PTS-negative isolates under laboratory
238 conditions.
239 A series of biochemical experiments were carried out to compare the
240 acidogenic and aciduric properties of SK36 and the constructed isogenic *manL*
241 mutant. First, PTS assays (Fig. 1C), which measure *in vitro* sugar
242 phosphorylation by permeabilized bacterial cells, showed a significant reduction
243 in the ability of the *manL* mutant to transport glucose or mannose, thus
244 confirming the predicted function of the glucose-PTS operon in which the *manL*
245 gene resides. Next, a pH drop experiment was performed using late-exponential

246 phase cultures prepared with BHI. When provided with 50 mM glucose, the *manL*
247 mutant showed a slightly slower rate of lowering the pH, but the final pH attained
248 by the mutant was slightly lower, by about 0.14 pH units at the 40-min mark, than
249 the wild type (Fig. 2A). The *manLComp* strain produced a resting pH comparable
250 to the *manL* mutant, suggesting that the difference among these strains may not
251 be biologically significant. However, when the same cultures were first frozen at -
252 80°C, thawed and then their optical density was normalized before the pH drop
253 assay, the *manL* mutant showed a much greater capacity to lower the
254 environmental pH than the wild type, dropping it at a faster rate and producing a
255 significantly lower resting pH at the end of a 1-hour assay (Fig. 2B). Similar
256 results were obtained when cells harvested from TY-Glc cultures were used in
257 pH drop (data not shown). These results suggested that the *manL* mutant was
258 better at maintaining viability and/or metabolic activity after a freeze/thaw cycle.
259 Furthermore, when SK36 and the *manL* mutant were assessed for aciduricity
260 by growing on acidified agar plates or acidified BHI broth (adjusted to pH 6.0 and
261 pH 5.5, respectively), there was little to no difference in growth phenotypes
262 between the mutant and the wild type under either condition (data not shown).
263 However, when these strains were subjected to acid killing by incubating in 0.1 M
264 glycine, pH 3.8, the wild type rapidly aggregated, whereas there was no obvious
265 evidence of aggregation in the suspension of the *manL* mutant throughout the 1-
266 h period. Since aggregation could greatly reduce the accuracy of CFU
267 enumeration, we did not assess survival at pH 3.8 by plating. However, both the

sensitivity to freezing and thawing and the aggregation differences between the wild-type and *manL* deletion strains point to differences in envelope integrity.

Next, the strains were cultured batch-wise in BHI, in which glucose is the primary carbohydrate source, or in TY prepared with glucose or lactose, and the final pH after ≥20 h of incubation were recorded. These pH measurements showed an intriguing pattern. In overnight TY-Glc cultures, the *manL* mutant achieved a significantly higher final pH than the wild type (Fig. 3A), whereas in BHI cultures the *manL* mutant had a slightly lower pH than the wild type (Fig. 3C). The pH measurements of *manLComp* cultures matched those of the wild type. Meanwhile, little difference in pH was seen among the three strains after overnight growth in TY-lactose (Fig. 3A). This medium-specific effect on final pH after ≥20 h of growth could suggest a potential impact of the glucose-PTS on the ability of the strains to produce alkali via the arginine deiminase (AD) system, which releases ammonia that neutralizes acids both inside and outside of the cells (27). This hypothesis was tested first by RT-qPCR measuring the levels of mRNA for *arcA*, encoding the arginine deiminase enzyme, in cells cultured in TY-Glc or BHI. The results (Fig. 3D) indeed showed a significant increase in expression of *arcA* associated with loss of *manL*. Importantly, in overnight TY-Glc cultures, pH measurements of an *arcA manL* double mutant were significantly lower than the mutant deficient in *manL* alone (Fig. 3B). Therefore, enhanced activities of the AD system were in large part responsible for the increased pH seen in TY-Glc cultures of the *manL* mutant. To reconcile this conclusion with the pH measurements from BHI cultures, we posited that the different impacts of

291 *manL* deletion were due to a lack of significant levels of free arginine in BHI. As a
292 simple test of this hypothesis, L-arginine was added to BHI medium at
293 supplemental concentrations of 1 mM and 5 mM before cultivation of these three
294 strains. The results (Fig. 3C) showed an arginine-dependent increase in final pH
295 in all cultures, with the *manL* mutant yielding higher pH than the wild type when 5
296 mM supplemental arginine was added. Collectively, these results demonstrated
297 significant roles of the glucose-PTS in regulating aciduricity and alkali generation,
298 thereby affecting the competitiveness of the commensal bacterium under acidic
299 conditions, such as those created by the fermentation of large amounts of
300 carbohydrates.
301
302 **The *manL* mutant produces more H_2O_2 and less lactate.** *S. sanguinis* is
303 considered a health-associated commensal and has antagonistic properties
304 toward the major etiologic agent of dental caries, *S. mutans*; with a primary
305 antagonistic factor being hydrogen peroxide (H_2O_2). When the *manL* deletion
306 mutant and its complemented derivative *manLComp* were tested for their abilities
307 to release H_2O_2 on agar plates, visualized as precipitation zones on Prussian
308 blue plates (28), the results showed that loss of *manL* significantly enhanced the
309 release of H_2O_2 by the bacterium (Fig. 4A). When tested in a plate-based
310 competition assay together with *S. mutans*, the *manL* mutant showed a
311 significantly increased ability to inhibit *S. mutans* UA159, relative to the wild-type
312 SK36 (Fig. 4B). The UA159 strain used in this study was a *perR*$^+$ stock obtained
313 from ATCC, as opposed to the UA159 derivative that carries a spontaneous

mutation in *perR* that truncates PerR and reduces sensitivity to H_2O_2 and oxidative stress in general (29). When *S. sanguinis* strains were each mixed with UA159 before being placed onto the agar plates, the *manL* mutant similarly outperformed its wild-type parent in competition against UA159, as quantified by CFU enumeration (data not shown). The *manLComp* strain behaved similarly to the *manL*$^+$ parent strain in these assays (Fig. S3). Consistent with the role of ManLMN in transporting glucose, both of these phenotypes depended on the presence of glucose (20 mM) and oxygen, and were not seen when lactose (10 mM) was used in place of glucose as the growth carbohydrate (Fig. 4). The *manL* mutant, however, showed enhanced H_2O_2 production on TY agar formulated with a combination of glucose and galactose, or with only galactose, GlcN, or GlcNAc (Fig. 4). As noted above, these four carbohydrates are transported primarily via the ManLMN PTS permease in closely related bacteria (30-32).

As H_2O_2 is generated by pyruvate oxidase (SpxB) during the conversion of pyruvate to acetyl phosphate (AcP) in the presence of oxygen, we reasoned that deletion of *manL* could have altered the flow of pyruvate in bacterial central metabolism (12). Under carbohydrate-rich and oxygen-limited conditions, streptococci are known to produce large quantities of lactate by reducing pyruvate, a reaction that is catalyzed by lactate dehydrogenase (LDH) and coupled to the conversion of NADH to NAD^+ (33). To test if enhanced shunting of pyruvate through SpxB might diminish lactate production, lactate levels were measured in the supernates of bacterial batch cultures prepared with TY medium supplemented with glucose or lactose as the carbohydrate source. The results

337 showed reduced lactate levels, by about 40%, in cultures of the *manL* mutant
338 grown on glucose, compared to the wild type grown on glucose (Fig. 1D); an
339 outcome supporting that pyruvate was directed away from lactate generation. On
340 the other hand, no significant differences in lactate accumulation were seen in
341 cultures grown on lactose. It is likely that reduced homolactic fermentation by the
342 *manL* mutant resulted in redirection from lactate production to acids with a higher
343 p*Ka*, e.g., acetate, or other non-acidic end products, such as ethanol and
344 acetoin, which may enhance the survival of *S. sanguinis* by increasing the
345 intracellular pH and reducing the amount of damage caused by low
346 environmental pH. However, this interpretation would not be entirely consistent
347 with the modestly lower environmental pH achieved by the *manL* mutant when
348 growing in BHI medium (Fig. 3C).
349
350 **Loss of *manL* alters central metabolism.** To further characterize the role of
351 the glucose-PTS in carbohydrate metabolism by *S. sanguinis*, RT-qPCR was
352 performed to measure the mRNA levels of genes involved in central metabolism
353 and related pathways in the *manL* mutant grown with glucose or lactose (Fig. 5
354 and Fig. S4). Consistent with the aforementioned phenotypes, transcriptional
355 analysis indicated that the *manL* mutant, when growing on glucose, had reduced
356 expression of the gene for lactate dehydrogenase (*ldh*). Also reduced was the
357 expression of *pykF* gene, encoding for pyruvate kinase, which converts PEP into
358 pyruvate with the concomitant generation of ATP. Reductions in mRNA levels of

359 *pykF* and *ldh* are indicative of decreases in glycolytic rate and homolactic
360 fermentation, respectively.
361 Conversely, the *manL* mutant displayed enhanced expression by genes in
362 oxidative pyruvate pathways that included *nox, spxB, pfl, acoB*, *pta,* and *ackA*.
363 NADH oxidase (NOX) is required for oxidation of NADH into NAD^+ in the
364 presence of oxygen, resulting in formation of H_2O. The levels of *pfl* mRNA, for a
365 pyruvate-formate lyase that catalyzes the conversion of pyruvate into acetyl-CoA
366 and formate, and *acoB* (SSA_1176), which belongs to the acetoin
367 dehydrogenase operon, were also higher. As a neutral product of pyruvate
368 catabolism, acetoin can be produced and released without influencing
369 cytoplasmic or environmental pH, or it can be converted by the acetoin
370 dehydrogenase complex into acetyl-CoA (34). Gene products of *pta* and *ackA*
371 are required for further metabolism of acetyl-CoA, leading to production of
372 acetate with concurrent generation of ATP. While SpxB is directly responsible for
373 oxidation of pyruvate with production of H_2O_2, Nox was found to be required for
374 optimal H_2O_2 release (35, 36). Enhanced expression of the genes for these
375 enzymes substantiated earlier observations of increased H_2O_2 release by the
376 *manL* mutant, as well as replacement of lactate by alternative end products, such
377 as acetate. In each case, the *manL* mutant showed significant changes in gene
378 expression when growing on glucose, but not on lactose, and the *manLComp*
379 strain produced the mRNAs of interest at levels comparable to the wild type (Fig.
380 S4).
381

382 **The *manL* mutant releases more pyruvate, but less eDNA.** Catabolite control
383 protein CcpA negatively regulates the expression of the pyruvate oxidase gene
384 *spxB* and production of H_2O_2 in *S. sanguinis* strain SK36 (20). However, the *ccpA*
385 mutant failed to show improved inhibition of *S. mutans* UA159 *in vitro*, a
386 phenotype that was attributed to overproduction and release of pyruvate, an
387 antioxidant that can scavenge H_2O_2 and thereby diminish its antagonism of *S.*
388 *mutans* (21). Since deletion of the glucose-PTS impedes growth on glucose, it
389 was reasoned that a *manL* mutant should experience a reduction in CCR, which
390 could lead to production of elevated levels of H_2O_2 (as noted in Fig. 4) and
391 perhaps even pyruvate. In contrast to a *ccpA* mutant, an increase in H_2O_2
392 secretion due to loss of *manL* was not evident when cells were grown on lactose,
393 but the effects were especially evident when glucose, galactose, GlcN, or
394 GlcNAc was the primary growth carbohydrate. In fact, the *ccpA* mutant failed to
395 show any difference in H_2O_2 secretion from the wild type when grown on
396 galactose or the amino sugars. It appeared that loss of *manL* affected H_2O_2
397 production more broadly than *ccpA* deficiency and the effects of mutations could
398 manifest differently depending on the growth carbohydrate.
399 Significantly, the *ccpA* mutant failed to inhibit UA159 in our plate assays, as
400 suggested previously (21), but the *manL* mutant inhibited UA159 moreso than
401 the wild type on all carbohydrates tested except lactose (Fig. 4B). We also
402 measured pyruvate levels in overnight TY-Glc batch cultures of the *manL* or *ccpA*
403 mutant and the results (Fig. 6A) showed significantly more pyruvate in *manL*
404 cultures (0.37 mM/OD_{600}) than both the WT (0.07 mM/OD_{600}) and the *ccpA*

mutant (0.17 mM/OD_{600}). No effect of either mutation was noted in cells grown on lactose. Monitoring of pyruvate release throughout the growth phases gave no indication that pyruvate was being actively reinternalized at any growth stage (Fig. 6BC); *S. mutans* actively reinternalizes pyruvate when it begins to enter stationary phase (37). The OD_{600} results (Fig. 6BC) from this experiment (also see Fig. S5A) revealed enhanced biomass of the *manL* mutant throughout the 24-h period. To explore the possibility that deletion of *manL* affected bacterial autolysis, extracellular DNA (eDNA) levels were measured in overnight TY-Glc cultures using SYTOX Green. Significantly lower eDNA levels were present in the cultures of the *manL* mutants than in cultures of the wild type (Fig. 6D), suggesting that the *manL* mutant lysed less than the wild type; when lysis of streptococci occurs, it is usually in stationary phase. Interestingly, a *manL ccpA* double mutant of SK36 produced pyruvate at levels comparable to the wild type (Fig. 6A). Furthermore, the *manL ccpA* double mutant showed a greater capacity to inhibit the growth of UA159 than the *ccpA* mutant (Fig. 4B). These results indicate that the ManL component of the glucose-PTS is capable of regulating central metabolism independently of CcpA.

Transcriptional analysis was again performed in order to better test this hypothesis. The results of the RT-qPCR (Fig. 5) showed that most genes involved in pyruvate metabolism were regulated in similar fashions in the *manL* and *ccpA* mutants, except for pyruvate dehydrogenase (*pdh*) and acetoin dehydrogenase genes. Specifically, whereas the *ccpA* mutant produced about 5 times more *pdhD* mRNA than the wild type, the *manL* mutant showed no

428 significant change in *pdhD* expression. The levels of *acoB* mRNA remained
429 largely unchanged in the *ccpA* mutant but were increased > 2-fold in the *manL*
430 mutant. Considering the significance of Pdh in metabolizing pyruvate under
431 aerobic conditions, its enhanced expression in the *ccpA,* but not in the *manL*
432 mutant, could provide an explanation for the higher levels of pyruvate being
433 detected in the glucose cultures of the *manL* mutant. In addition, both the *ccpA*
434 and the *manL* mutants produced significantly lower *ldh* mRNA than the wild type,
435 consistent with the apparent redirection of pyruvate away from lactate production.
436 It was not immediately clear why such high levels of extracellular pyruvate did not
437 suppress H_2O_2-mediated antagonism of UA159 by the *manL* mutant (Fig. 4B).
438 However, we hypothesized that accumulation of pyruvate itself could be a
439 contributing factor to the enhanced fitness of the *manL* mutant in acidic
440 environments and when the levels of H_2O_2 were elevated, especially in
441 consideration that H_2O_2 can trigger autolysis and eDNA release in *S. sanguinis*
442 (26, 38). Aside from being an antioxidant, metabolism of pyruvate via the
443 oxidative pathways should yield additional ATP, which is beneficial to
444 persistence, especially for maintaining pH homeostasis via the activity of F_1F_o-
445 ATPase (39). Thus, the enhanced competitive fitness of a *manL* mutant of *S.*
446 *sanguinis* may be attributable to a variety of factors that influence antagonism
447 against *S. mutans*, as well as survival of *S. sanguinis* in the presence of *S.*
448 *mutans* and its antagonistic products.
449

Exogenous pyruvate benefits SK36. To test the effects of pyruvate on the fitness of *S. sanguinis*, SK36 was inoculated in BHI with or without 5 mM pyruvate and incubated overnight (≥ 20 h) before the cultures were diluted and enumerated for CFUs on agar plates. At the same time, the cultures were diluted (1:100) into TY-Glc with and without 5 mM pyruvate before growth was monitored. Strain UA159 of *S. mutans* was included for comparison, as it is known to be highly aciduric. In both assays, inclusion of pyruvate in overnight BHI cultures significantly enhanced the persistence of SK36, as assessed by CFU (P <0.05, Fig. 7A) and growth rate of subcultures in TY-Glc (Fig. 7B). Addition of pyruvate in TY-Glc also enhanced the growth rate of SK36 that was diluted from overnight cultures prepared without pyruvate (Fig. 7C). When the *manL* mutant of SK36 was cultured with added pyruvate, it too produced enhanced CFU counts, although its CFU counts were greater than the wild type with or without addition of pyruvate (Fig. 7A). By contrast, *S. mutans* UA159 showed no statistically significant change in either overnight viable counts or growth characteristics of TY-Glc cultures in response to the presence of 5 mM pyruvate. These results suggested that the presence of pyruvate in the environment could benefit the persistence of the commensal relative to *S. mutans*.

In light of the presence of *manL* mutations and the abundance of other SNPs (Table S1) detected in our two SK36 stocks, we obtained a third stock of SK36 from ATCC and constructed a *manL* deletion mutant for comparison. Studies of this new mutant in persistence, antagonism of UA159, release of H_2O_2 and

pyruvate, as well as other growth characteristics showed effects highly similar to the *manL* mutants created using the other two strains of SK36 (Fig. S5 and data not shown). All three SK36 stocks also displayed highly similar phenotypes in these assays (Fig. S5). To our surprise, WGS indicated that the ATCC SK36 stock (here designated MMZ1922) carries nearly identical SNPs (totaling 116, Table S1) to those of the aforementioned two stocks, raising the possibility that the genome sequence of SK36 deposited at GenBank was derived from a strain that is significantly different from what is available from ATCC and what is being used by at least two oral streptococcus research groups. The basis for the differences between the sequence deposited in GenBank and that of the strains used here is not known, but could be accounted for by advances in sequencing technology since the original sequence was deposited. Meanwhile, an analysis using multi-locus sequence typing (Fig. S6) placed both the GenBank sequence and the assembled genome of the ATCC stock (MMZ1922) within the species of *S. sanguinis* as recently determined by sequencing and phylogenomic analysis of 25 low-passage clinical isolates of *S. sanguinis* (40).

Detection of extracellular pyruvate in cultures of oral bacteria. Detection of spontaneous *manL* mutants in SK36 raised the possibility that isolates with similar genetic lesions could exist in nature, and those isolates would likely display similar phenotypes, including increased excretion of pyruvate. This hypothesis was tested using two cohorts of oral bacterial isolates made available from previous studies, including 63 commensal isolates from mostly caries-free

donors (40) and 96 clinical isolates from both caries-free and caries-active subjects (41). When grown with TY-glucose or TY-lactose overnight in an aerobic atmosphere, a majority (~90%) of these bacteria did not produce significant levels of pyruvate in their culture supernates. However, a total of 16 strains had significant levels of pyruvate (>0.15 mM/OD_{600}) in their culture media 20 h post inoculation (Fig. S7A). These pyruvate-positive strains included multiple oral streptococcal species, from both caries-free and caries-active hosts. The issue of whether the original stocks of these isolates contained subpopulations of *manL* mutants was not evaluated because of the unrealistic scope of such an undertaking. Still, it must be considered that the results could reflect the sum of heterogeneous behaviors of genetically different subpopulations, the proportions of which may differ by isolate.

We next cultivated unstimulated whole saliva samples obtained from four healthy donors in a semi-defined medium containing various carbohydrates (42), including glucose, fructose, galactose, GlcN, GlcNAc, lactose, sucrose, or maltose, then measured pyruvate levels in the supernates. Out of four saliva samples, three produced significantly higher pyruvate levels on certain carbohydrates, with each showing a different profile in response to the primary carbohydrate in the medium (Fig. S7B). These latter results demonstrate that pyruvate can accumulate in complex populations of oral bacteria that more closely mimic the composition of the salivary microbiome in a carbohydrate-dependent manner.

519

520 Discussion

521 In addition to acidogenicity, acid tolerance (aciduricity) is a key attribute of
522 organisms that contribute to the initiation and progression of dental caries. The
523 continued metabolic activities of acid-tolerant bacteria under acidic conditions
524 shifts the ecological balance away from health-associated, acid-sensitive
525 commensals, enhancing the virulence of the biofilms. While much attention has
526 been paid to the aciduricity and acid tolerance response (ATR) by mutans
527 streptococci, especially *S. mutans*, limited information is available regarding
528 many of the abundant commensal streptococci. These bacteria make up the bulk
529 of the dental microbiome and remain part of the biofilm even during significant
530 caries events (43), and many are capable of fermenting carbohydrates as
531 efficiently or superior to the etiological agents of caries (44, 45). Here we
532 reported the identification of spontaneous mutants of *S. sanguinis* SK36
533 deficient, in whole or in part, in the ManL component of the glucose-PTS that
534 showed improved fitness in stationary phase and acidic conditions. These
535 phenotypic changes coincided with a shift of central carbon metabolism away
536 from lactate generation in favor of pyruvate-oxidizing enzymes, resulting in
537 increased secretion of H_2O_2 and pyruvate, and increased arginine deiminase
538 activity. As such, the *manL* mutant of SK36 not only outcompeted its isogenic
539 parent in stationary phase, but also showed significantly greater competitiveness
540 against *S. mutans* on agar plates. As the conditions that likely contributed to the
541 emergence of these mutants - growth in rich media containing high

542 concentrations of glucose and the resultant low pH - are also expected in caries-
543 conducive dental biofilms, our findings could have relevance in understanding the
544 role of the glucose-PTS in regulating bacterial metabolism in ways that affect the
545 overall aciduricity of dental biofilms. The findings also give rise to the hypothesis
546 that there may be selection for mutants of commensal streptococci with defects
547 in the ManL component of the PTS under cariogenic conditions that allow these
548 variants to better survive, and perhaps even contribute to, cariogenic conditions.
549 Why is the *manL* mutant better at surviving in an acidic environment? When
550 using fast-growing, exponential phase cells, pH drop and acid killing assays did
551 not reveal the *manL* mutant to be more acid tolerant than the wild type.
552 Nevertheless, it was clear that the mutant fared better under certain acidic
553 conditions and was better able to maintain viability following a freeze-thaw cycle.
554 We were also able to show that after prolonged incubation in the stationary
555 phase, either on agar plates or in liquid cultures, the *manL* mutant had
556 significantly greater viability than the wild type. It is possible that the most
557 pronounced phenotype of the *manL* deletion occurs during the stationary phase,
558 when the pH happens to be the lowest. For example, the *manL* mutant could
559 have reduced propensity for autolysis, as our results have indicated (Fig. 6D),
560 and it is known that extreme pH and/or high H_2O_2 levels can trigger cells to
561 undergo autolysis (26, 38, 46). Based on qRT-PCR data, we hypothesize that a
562 few mechanisms could be responsible for enhanced fitness of mutants lacking an
563 intact ManLMN permease: i) altered metabolic end products, namely less lactate
564 and more acetate, perhaps even change in acetoin levels, result in elevated

565 intracellular pH with less damage to critical cellular components; ii) enhanced
566 activities in pyruvate oxidative pathways provide more efficient production of
567 ATP; iii) increased expression of the AD system allows cells to catabolize
568 arginine, which benefits the bacterium both bioenergetically through creation of
569 ATP and improved pH homeostasis; and iv) reduced LDH activity creates a
570 surplus of pyruvate, which could scavenge H_2O_2 or provide a substrate to extend
571 ATP production or be used for biogenesis pathways that enhance persistence
572 under stressful conditions (e.g. membrane remodeling). Though not widespread
573 in streptococci, *S. sanguinis* genome harbors putative genes required for
574 gluconeogenesis which converts pyruvate into metabolic intermediates and
575 precursors required for critical biogenesis pathways (16, 17). Indeed, pyruvate
576 has been shown to resuscitate VBNC (viable but not culturable) *E. coli* cells by
577 promoting macromolecular biosynthesis (47). Intracellular pyruvate could also
578 potentially serve as a signal that alters gene regulation in favor of acid resistance
579 (48). Further study on this subject, e.g. analysis at the systems level via
580 proteomics or metabolomics, will be needed for confirmation of these theories.
581 Recently *S. mutans* was shown to release pyruvate as an overflow metabolite,
582 which could then be reinternalized via dedicated transporters once excess
583 glucose in the environment is depleted (37). *S. mutans* possesses two
584 holin/antiholin-like proteins, LrgAB, that are responsible for transporting pyruvate
585 at the start of stationary phase. Research has suggested the existence of
586 additional transporters or mechanisms for pyruvate to impact the growth of *S.*
587 *mutans* (49). The genome of *S. sanguinis* lacks homologues of either gene, but

588 *S. sanguinis* and other *spxB*-encoding species do release pyruvate in varying
589 amounts to the surroundings, which can decrease the damaging effects of H_2O_2
590 (21). Our measurements of exogenous pyruvate did not seem consistent with an
591 highly active mechanism for reinternalization of pyruvate in SK36 (Fig. 6BC), yet
592 addition of exogenous pyruvate improved bacterial persistence in overnight
593 cultures (Fig. 7; Fig. S5B). Relative to the control, cultures with added pyruvate
594 showed enhanced viability when sub-cultured. Meanwhile, pyruvate treatment
595 failed to enhance the final OD_{600} or pH of overnight cultures, however it did
596 reduce eDNA release by a modest amount (23%, P <0.05; Fig. S5ACD). Again,
597 these results run counter to the existence of a dedicated pyruvate transporter for
598 *S. sanguinis*, however they do not rule out that pyruvate uptake occurs
599 nonspecifically. Alternatively, as H_2O_2 can diffuse freely through cell membranes,
600 pyruvate could impact bacterial physiology simply by reacting with H_2O_2 in the
601 environment.

602 How does the glucose-PTS regulate multiple metabolic pathways? Excess
603 amounts of exogenous glucose can inhibit oxidative phosphorylation in favor of
604 ethanol or lactate fermentation; a phenomenon termed the Crabtree effect in
605 eukaryotic systems, e.g. yeast and tumor cells (50), or carbon catabolite
606 repression (CCR) in facultatively anaerobic bacteria. The genetic mechanism
607 responsible for this effect in most Gram-positive bacteria has been attributed to
608 catabolite control protein CcpA, although recent research has pointed to other
609 PTS-specific, CcpA-independent mechanisms, particularly in streptococci (19,
610 51-54). Our transcription analysis (Fig. 5) showed altered expression, due to loss

of *manL,* in many central metabolic pathways, for which we envisioned three possible mechanisms. First, loss of *manL*, with the accompanying reduction in PTS activity could significantly impede PTS-mediated glucose influx, thereby reducing the steady state concentrations of the critical metabolic intermediates G-6-P and F-1,6-bP. In turn, the enzymatic activity of LDH, which is known to be allosterically activated by F-1,6-bP (10), also decreases. As LDH activity is critical to maintaining the NAD^+/NADH balance, this change would likely affect the expression of multiple genes responsive to intracellular redox balance (36, 55), including *ldh* itself (56). This rationale could likewise be applied to cells growing in GlcN or GlcNAc, the catabolism of which yields F-6-P and subsequently F-1,6-bP. However, this would not apply in the case of galactose metabolism, as neither the tagatose pathway nor the Leloir pathway yields these intermediates. The second possibility involves CcpA-dependent regulation of gene expression. Since the ManLMN permease is the primary transporter of a number of monosaccharides, its activity is needed to sustain a certain level of energy intermediates, namely G-6-P, F-1,6-bP, and ATP, that are crucial to the function of the major catabolite regulator CcpA. A recent study of the CcpA regulon in *S. sanguinis*, performed using cells cultured in rich-medium, has revealed the various pathways and cellular functions that are controlled by CcpA (18). This list included *manL*, *pfl, spxB,* and several hundred other genes. The third scenario would be CcpA-independent. Our transcription analysis (Fig 5) indicated that *ldh*, *nox*, the *arc* operon, and the *pdh* operon are affected by the deletion of *manL* gene, however they were not identified as part of CcpA regulon

in the aforementioned study (18); despite the fact that CcpA does control *arc* gene expression in the metabolically similar bacterium *S. gordonii* (8). Compared to the *ccpA* mutant, the *manL* mutant showed significantly more drastic effects on H_2O_2 production when growing on glucose, galactose, GlcN, GlcNAc, or a combination of glucose and galactose. Except for glucose or glucose and galactose, the *ccpA* mutant actually behaved much like the wild type (Fig. 4). Likewise, production of H_2O_2 by the *manL ccpA* double mutant matched that of the *ccpA* mutant in most cases, but was greater than that of the *ccpA* mutant on the amino sugars. Further, while a *nox* mutant showed a greatly reduced capacity to release H_2O_2, a *manL nox* double mutant produced more H_2O_2 than the *nox* mutant did under most conditions (Fig. 4). Although *spxB* is under the direct control of CcpA, our findings strongly support a CcpA-independent, PTS-specific pathway for regulating SpxB and related activities. A recent study on glucose-dependent regulation of *spxB* in *S. sanguinis* and *S. gordonii* identified significant distinctions between these two commensals in their response to availability of glucose (20), suggesting the presence of regulatory mechanisms beyond CcpA that could control pyruvate metabolism. We also previously reported that the glucose-PTS was capable of exerting catabolic control, independently of CcpA, over a fructanase gene (*fruA*) in *S. gordonii* (53).

In a caries-conducive dental plaque, rapid fermentation of dietary carbohydrates by lactic acid bacteria creates both detrimentally low pH and decreases the amount of carbohydrate available to commensals. These *in vivo* conditions do resemble that of a post exponential-phase batch culture whenever

carbohydrate-rich media are used to grow streptococci. Such conditions could select for the *manL* mutations as the populations adapt to the stresses. In line with this reasoning, we have provided evidence supporting the existence of bacteria or mutants with decreased LDH activity and increased pyruvate oxidation and excretion within laboratory and clinical isolates, and shown variability in pyruvate production with a small set of *ex vivo* cultures grown from four different saliva donors. It is also understood that pyruvate exists in the oral cavity at varying levels, dependent upon the metabolic status and the functional makeup of the microbiome (57, 58). We recognize the fact that many of these isolates and multi-species cultures need further characterization in their metabolic capacities, as well as genetic composition. Nonetheless, the presence of these mutants in populations supports that there are advantages to the *manL* mutation, and perhaps other not-yet-identified mutations, under conditions such as those associated with caries development. Further, most of these bacteria are likely considered commensals, yet the impact of the physiological activities of these mutants on the dental microbiome remains unexplored. For example, *S. mutans* and other bacteria capable of actively transporting pyruvate could utilize exogenous pyruvate as a nutrient or for protection from oxidative stress. Previous studies in *S. mutans* show that the pyruvate dehydrogenase pathway is induced under starvation, contributing to aciduricity and long-term survival of the bacterium (59, 60). Further research into the role of PTS in pyruvate metabolism and its ecological impact to oral bacteria could reveal novel understandings in mechanisms that contribute to microbial homeostasis and oral health. Such

knowledge of fundamental differences in the metabolism of carbohydrates by commensals and caries pathogens could be applied to promote health-associated biofilm communities.

Materials and methods

Bacterial strains and culture conditions. Three different stocks of *S. sanguinis* SK36 and their mutant derivatives, and *S. mutans* strain UA159 (Table 1) were maintained on BHI (Difco Laboratories, Detroit, MI) agar plates or Tryptone-yeast extract (TY, 3% Tryptone and 0.5% yeast extract) agar plates, each supplemented with 50 mM potassium phosphate, pH 7.2. Antibiotics including kanamycin (Km, 1 mg/mL), erythromycin (Em, 10 μg/mL), and spectinomycin (Sp, 1 mg/mL) were used in agar plates for the purpose of selecting for antibiotic-resistant transformants. BHI liquid medium was routinely used for preparation of batch starter cultures, which were then diluted into BHI, TY, or the chemically-defined medium FMC (61) modified to contain various carbohydrates at specified amounts. Cultures or the agar plates were incubated at 37°C in an aerobic environment with 5% CO_2. Bacterial cultures were harvested at specified growth phases by centrifugation at 15,000 × *g* at 4°C for 10 min, or at room temperature for 2 min. The cells or the supernates were used immediately for biochemical reactions or stored at -80°C. For the purpose of studying growth characteristics, bacterial starter cultures were diluted into FMC or TY containing various carbohydrates and loaded onto a Bioscreen C system, where wells were overlaid with mineral oil, and cultures were maintained at 37°C.

Chromosomal DNA was extracted from bacterial cells using a Wizard Genomic DNA purification kit (Promega, Madison, WI), and submitted to MiGS (Microbial Genome Sequencing Center, Pittsburgh, PA; https://www.migscenter.com/) for WGS (Illumina) analysis and variant calling (Table S1). The coverage of these WGS genomes ranged between 40- to 50- fold. The high-throughput data of the genomic sequence of ATCC BAA-1455 (MMZ1922) were deposited in the Sequence Read Archive (SRA) and assigned an accession number PRJNA726918 (more information is available from the corresponding author upon request). To analyze the phylogenetic relationship of BAA-1455 with other streptococci, a multi-locus sequence typing (MLST) was performed using the genomes of *S. sanguinis* SK36 and *S. mutans* UA159 from GenBank, the ABySS assembly (14 Contigs) of MMZ1922 (62), along with the genomes of 25 low-passage *S. sanguinis* isolates and numerous clinical isolates of other streptococci obtained from our latest research (40).

Construction of deletion mutants and complementing derivatives. An allelic exchange strategy (63) was modified to allow easy replacement of the target gene, e.g., *manL*, with multiple antibiotic markers (knockouts), and for the purpose of genetic complementation (*manLComp*), knocking-in of the wild-type gene (*manL*) in place of the antibiotic marker at the original site (26). Each recombinant event was facilitated by transformation of naturally competent bacterium using a linear DNA comprised of two homologous fragments, each at least 1 kbp in length, flanking an antibiotic marker (for knockouts) or a wild-type

726 copy of *manL* sequence followed by a different antibiotic marker (for knock-ins).
727 For the amplification of the upper flanking fragment, a 27-nucleotide sequence
728 (sequence A) was added to the front of the regular reverse primer (Table S2,
729 underlined in primer Ssa1918-2GA); and for the lower flanking fragment, a 30-
730 nucleotide sequence (sequence B) was added to the front of the regular forward
731 primer (underlined in primer Ssa1918-3GA). For PCR-amplification of antibiotic
732 markers, including Km, Em and Sp, specific primers were designed for the
733 integration of sequences A and B into the 5'- and 3'- ends, respectively, of each
734 fragment (Table S2, labelled as "Marker for GA"). A mutator DNA for knockouts
735 was created from two flanking DNA fragments and an antibiotic marker of choice,
736 each at approximately 100 ng, using a 12-µL Gibson Assembly (GA) reaction
737 (purchased from NEB or prepared in house) by incubation at 50°C for 1 h.
738 Competent bacterial cells were induced by the use of a synthetic competence-
739 stimulating peptide (CSP, by ICBR at the University of Florida) previously
740 identified for *S. sanguinis* (64).
741 For complementation via knocking-in, a different "-2GA" primer
742 (Ssa1918_manL_Comp-2GA) was designed and used together with the original
743 forward primer (Ssa1918-1), so that the upper fragment now contained the wild-
744 type gene in addition to the flanking sequence, ending with the same overlapping
745 sequence A. This new fragment, the original lower fragment and an antibiotic
746 marker of choice (different from the one replacing *manL*) were then ligated
747 together via GA reaction to create a DNA to restore a wild-type *manL* operon.

Each strain was confirmed by PCR using two outmost primers (with names ending in "-1" and "-4"; Table S2), followed by Sanger sequencing to ensure that no mutations were introduced into the target or flanking sequences. The primers used in sequencing, GA-Seq-5' and GA-Seq-3', were derived from the sequences A and B, respectively, each facing outward from the antibiotic marker, thus can be used for all mutants constructed the same way.

PTS assay and pH drop. The capacity of the bacterium to transport carbohydrates and to lower environmental pH as a result of carbohydrate fermentation was assessed using the PTS assay (65, 66) or a pH drop assay, respectively, as previously described (39, 66).

RNA extraction and RT-qPCR. Bacterial cultures (5 to10 mL) from mid-exponential phase (OD_{600} = 0.5-0.6) were harvested and treated with RNAprotect reagent (Qiagen, Germantown, MD), and the cell pellet, if not immediately processed, was stored at -20°C. Bacterial cells were resuspended in a lysis buffer (Qiagen), together with an equal volume of acidic phenol and similar volume of glass beads, and disrupted by beadbeating for 1 min. After 10 min of centrifugation at 15,000× *g* at room temperature, the clarified aqueous layer was removed and processed using an RNeasy mini kit (Qiagen) for extraction of total RNA. While loaded on membrane of the centrifugal column, the RNA sample was treated with RNase-free DNase I solution (Qiagen), twice, to remove genomic DNA contamination.

771 To synthesize cDNA, 0.5 µg of each RNA sample was used in a 10-µL reverse
772 transcription reaction set up using the iScript Select cDNA synthesis kit (Bio-
773 Rad), together with gene-specific reverse primers (Table S2) used at 200 nM
774 each. Primer for the housekeeping gene *gyrA* was used as an internal control in
775 all cases (67). After a 10-fold dilution with water, the cDNA was used as a
776 template in a quantitative PCR (qPCR) reaction prepared using a SsoAdvanced
777 Universal SYBR Green Supermix and cycled on a CFX96 Real-Time PCR
778 Detection System (Bio-Rad), following the supplier's instructions. Each strain was
779 represented by three biological replicates and each cDNA sample was assayed
780 at least twice in the qPCR reaction. The relative abundance of each mRNA was
781 calculated against the housekeeping gene using a ΔΔCq method (68).
782
783 **H_2O_2 measurement and plate-based competition assay.** The relative capacity
784 of each strain to produce H_2O_2 and to compete against *S. mutans* was studied by
785 following previously published protocols with minor changes. H_2O_2 production
786 was assessed using an indicator agar plate on the basis of Prussian blue
787 formation (21, 28). Briefly, a tryptone (3%)-yeast extract (0.5%) agar (1.5%) base
788 was prepared with the addition of $FeCl_3.6H_2O$ (0.1%) and potassium
789 hexacyanoferrate (III) (0.1%). After autoclaving, glucose or other carbohydrates
790 were added at the specified amounts before pouring plates. Each strain was
791 cultivated overnight in BHI medium and dropped onto the agar surface, then
792 incubated for >20 h to allow bacterial growth and development of Prussian blue
793 precipitation. Each strain was tested at least three times, with 2 plates each time.

794 Plate-based inhibition assays (42) were carried out to test the interactions
795 between *S. sanguinis* and *S. mutans* UA159 on various carbohydrate sources
796 using TY-agar as the base medium. Overnight cultures of *S. sanguinis* strains
797 were dropped onto the agar first, incubated for 24 h at 37°C in a 5% CO_2 aerobic
798 incubator, followed by spotting of *S. mutans* UA159 in close proximity to the *S.*
799 *sanguinis* colony. Plates were incubated for another day before photographing.
800 Each interaction was tested at least three times.
801
802 **Lactate and pyruvate measurement.** Bacterial cultures were prepared by
803 diluting overnight BHI cultures at 1:50 into TY medium supplemented with 20 mM
804 glucose, then incubated at 37°C in an aerobic incubator maintained with 5% CO_2.
805 At the specified time or phase of growth, aliquots of bacterial cultures were taken
806 for optical density measurement (OD_{600}), or spun down using a tabletop
807 centrifuge (14,000× *g*, 2 min), with supernates being removed for assays or
808 stored at -20°C. Lactate levels in the culture supernates were measured using a
809 lactate assay kit (LSBio, Seattle, WA), following the protocols provided by the
810 supplier.
811 To measure pyruvate levels in the same cultures, we adopted an LDH-
812 catalyzed reaction that coupled the reduction of pyruvate with the oxidation of
813 NADH with monitoring of the optical density at 340 nm (OD_{340}). The assay was
814 performed by mixing 10 µL sample and 90 µL of enzyme solution, which included
815 10 Units/mL of lactate dehydrogenase (Sigma) and 100 µM NADH in a 100 mM
816 sodium-potassium phosphate buffer (pH 7.2) supplemented with 5 mM $MgCl_2$.

The reaction was incubated at room temperature for 10 min before spectrometry, with the light source set at UV range. To rule out the influence to the assay by background NADH-oxidizing activities in bacterial cultures, a control without addition of LDH was included for each sample. A sodium pyruvate standard in the range of 0.05 to 0.6 mM was prepared freshly in TY base medium. The final measurements of pyruvate concentration were normalized against the optical density (OD_{600}) of each culture. An earlier approach (69) to quantifying pyruvate using a commercial kit was not used due to the presence in samples of H_2O_2 that interferes with the reaction. Collection of saliva was carried out according to an established procedure (IRB201500497 at University of Florida) described elsewhere (42).

Acknowledgements

This work was supported by DE12236 from the United States National Institute of Dental and Craniofacial Research. We thank Dr. Jacqueline Abranches for providing a subset of the clinical isolates of oral streptococci used in this study.

References

1. Takahashi N, Nyvad B. 2011. The role of bacteria in the caries process: ecological perspectives. J Dent Res 90:294-303.
2. Beighton D. 2005. The complex oral microflora of high-risk individuals and groups and its role in the caries process. Community Dent Oral Epidemiol 33:248-55.

840 3. Peterson SN, Snesrud E, Liu J, Ong AC, Kilian M, Schork NJ, Bretz W.
841 2013. The dental plaque microbiome in health and disease. PLoS One
842 8:e58487.
843 4. Liu YL, Nascimento M, Burne RA. 2012. Progress toward understanding
844 the contribution of alkali generation in dental biofilms to inhibition of dental
845 caries. Int J Oral Sci 4:135-40.
846 5. Cheng X, Redanz S, Cullin N, Zhou X, Xu X, Joshi V, Koley D, Merritt J,
847 Kreth J. 2018. Plasticity of the pyruvate node modulates hydrogen
848 peroxide production and acid tolerance in multiple oral Streptococci. Appl
849 Environ Microbiol 84.
850 6. Kreth J, Zhang Y, Herzberg MC. 2008. Streptococcal antagonism in oral
851 biofilms: *Streptococcus sanguinis* and *Streptococcus gordonii* interference
852 with *Streptococcus mutans*. J Bacteriol 190:4632-40.
853 7. Redanz S, Cheng X, Giacaman RA, Pfeifer CS, Merritt J, Kreth J. 2018.
854 Live and let die: Hydrogen peroxide production by the commensal flora
855 and its role in maintaining a symbiotic microbiome. Mol Oral Microbiol
856 33:337-352.
857 8. Zeng L, Dong Y, Burne RA. 2006. Characterization of *cis*-acting sites
858 controlling arginine deiminase gene expression in *Streptococcus gordonii*.
859 J Bacteriol 188:941-9.
860 9. Postma PW, Lengeler JW, Jacobson GR. 1993.
861 Phosphoenolpyruvate:carbohydrate phosphotransferase systems of
862 bacteria. Microbiol Rev 57:543-94.

10. Garvie EI. 1980. Bacterial lactate dehydrogenases. Microbiol Rev 44:106-39.

11. Ritchey TW, Seely HW, Jr. 1976. Distribution of cytochrome-like respiration in streptococci. J Gen Microbiol 93:195-203.

12. Willenborg J, Goethe R. 2016. Metabolic traits of pathogenic streptococci. FEBS Lett 590:3905-3919.

13. Burne RA. 1998. Oral streptococci... products of their environment. J Dent Res 77:445-52.

14. Kreth J, Giacaman RA, Raghavan R, Merritt J. 2017. The road less traveled - defining molecular commensalism with *Streptococcus sanguinis*. Mol Oral Microbiol 32:181-196.

15. Kilian M, Mikkelsen L, Henrichsen J. 1989. Taxonomic study of Viridans Streptococci: Description of *Streptococcus gordonii* sp. nov. and emended descriptions of *Streptococcus sanguis* (White and Niven 1946), *Streptococcus oralis* (Bridge and Sneath 1982), and *Streptococcus mitis* (Andrewes and Horder 1906). International Journal of Systematic and Evolutionary Microbiology 39:471-484.

16. Valdebenito B, Tullume-Vergara PO, González W, Kreth J, Giacaman RA. 2018. *In silico* analysis of the competition between *Streptococcus sanguinis* and *Streptococcus mutans* in the dental biofilm. Molecular Oral Microbiology 33:168-180.

17. Xu P, Alves JM, Kitten T, Brown A, Chen Z, Ozaki LS, Manque P, Ge X, Serrano MG, Puiu D, Hendricks S, Wang Y, Chaplin MD, Akan D, Paik S,

886 Peterson DL, Macrina FL, Buck GA. 2007. Genome of the opportunistic
887 pathogen *Streptococcus sanguinis*. J Bacteriol 189:3166-3175.
888 18. Bai Y, Shang M, Xu M, Wu A, Sun L, Zheng L. 2019. Transcriptome,
889 phenotypic, and virulence analysis of *Streptococcus sanguinis* SK36 wild
890 type and its CcpA-null derivative (ΔCcpA). Front Cell Infect Microbiol
891 9:411.
892 19. Gorke B, Stulke J. 2008. Carbon catabolite repression in bacteria: many
893 ways to make the most out of nutrients. Nat Rev Microbiol 6:613-24.
894 20. Redanz S, Masilamani R, Cullin N, Giacaman RA, Merritt J, Kreth J. 2018.
895 Distinct regulatory role of carbon catabolite protein A (CcpA) in oral
896 streptococcal *spxB* expression. J Bacteriol 200.
897 21. Redanz S, Treerat P, Mu R, Redanz U, Zou Z, Koley D, Merritt J, Kreth J.
898 2020. Pyruvate secretion by oral streptococci modulates hydrogen
899 peroxide dependent antagonism. Isme j 14:1074-1088.
900 22. Zeng L, Burne RA. 2020. Molecular mechanisms controlling fructose-
901 specific memory and catabolite repression in lactose metabolism by
902 *Streptococcus mutans*. Mol Microbiol n/a:70-83.
903 23. Vadeboncoeur C, Pelletier M. 1997. The phosphoenolpyruvate:sugar
904 phosphotransferase system of oral streptococci and its role in the control
905 of sugar metabolism. FEMS Microbiol Rev 19:187-207.
906 24. Taylor DE. 1999. Bacterial tellurite resistance. Trends Microbiol 7:111-5.

907 25. Dong Y, Chen YY, Burne RA. 2004. Control of expression of the arginine
908 deiminase operon of *Streptococcus gordonii* by CcpA and Flp. J Bacteriol
909 186:2511-4.
910 26. Zheng L, Chen Z, Itzek A, Ashby M, Kreth J. 2011. Catabolite control
911 protein A controls hydrogen peroxide production and cell death in
912 *Streptococcus sanguinis*. J Bacteriol 193:516-26.
913 27. Burne RA, Marquis RE. 2000. Alkali production by oral bacteria and
914 protection against dental caries. FEMS Microbiol Lett 193:1-6.
915 28. Saito M, Seki M, Iida K-i, Nakayama H, Yoshida S-i. 2007. A novel agar
916 medium to detect hydrogen peroxide-producing bacteria Based on the
917 prussian blue-forming reaction. Microbiology and Immunology 51:889-892.
918 29. Kajfasz JK, Zuber P, Ganguly T, Abranches J, Lemos JA. 2021. Increased
919 oxidative stress tolerance of a spontaneously-occurring *perR* gene
920 mutation in *Streptococcus mutans* UA159. J Bacteriol
921 doi:10.1128/jb.00535-20.
922 30. Abranches J, Chen YY, Burne RA. 2003. Characterization of
923 *Streptococcus mutans* strains deficient in EIIAB^{Man} of the sugar
924 phosphotransferase system. Appl Environ Microbiol 69:4760-9.
925 31. Moye ZD, Burne RA, Zeng L. 2014. Uptake and metabolism of N-
926 acetylglucosamine and glucosamine by *Streptococcus mutans*. Appl
927 Environ Microbiol 80:5053-67.

928 32. Zeng L, Das S, Burne RA. 2010. Utilization of lactose and galactose by
929 *Streptococcus mutans*: transport, toxicity, and carbon catabolite
930 repression. J Bacteriol 192:2434-44.
931 33. Iwami Y, Abbe K, Takahashi-Abbe S, Yamada T. 1992. Acid production by
932 streptococci growing at low pH in a chemostat under anaerobic conditions.
933 Oral Microbiol Immunol 7:304-8.
934 34. Xiao Z, Xu P. 2007. Acetoin metabolism in bacteria. Crit Rev Microbiol
935 33:127-40.
936 35. Zheng LY, Itzek A, Chen ZY, Kreth J. 2011. Oxygen dependent pyruvate
937 oxidase expression and production in Streptococcus sanguinis. Int J Oral
938 Sci 3:82-9.
939 36. Ge X, Yu Y, Zhang M, Chen L, Chen W, Elrami F, Kong F, Kitten T, Xu P.
940 2016. Involvement of NADH oxidase in competition and endocarditis
941 virulence in *Streptococcus sanguinis*. Infect Immun 84:1470-1477.
942 37. Ahn SJ, Deep K, Turner ME, Ishkov I, Waters A, Hagen SJ, Rice KC.
943 2019. Characterization of LrgAB as a stationary phase-specific pyruvate
944 uptake system in *Streptococcus mutans*. BMC Microbiol 19:223.
945 38. Kreth J, Vu H, Zhang Y, Herzberg MC. 2009. Characterization of hydrogen
946 peroxide-induced DNA release by *Streptococcus sanguinis* and
947 *Streptococcus gordonii*. J Bacteriol 191:6281-91.
948 39. Bender GR, Sutton SV, Marquis RE. 1986. Acid tolerance, proton
949 permeabilities, and membrane ATPases of oral streptococci. Infect Immun
950 53:331-338.

951 40. Velsko IM, Chakraborty B, Nascimento MM, Burne RA, Richards VP.
952 2018. Species designations belie phenotypic and genotypic heterogeneity
953 in oral streptococci. mSystems 3:e00158-18.
954 41. Garcia BA, Acosta NC, Tomar SL, Roesch LFW, Lemos JA, Mugayar
955 LCF, Abranches J. 2021. Association of *Streptococcus mutans* harboring
956 bona-fide collagen binding proteins and *Candida albicans* with early
957 childhood caries recurrence. medRxiv
958 doi:10.1101/2021.02.28.21252629:2021.02.28.21252629.
959 42. Chen L, Chakraborty B, Zou J, Burne RA, Zeng L. 2019. Amino sugars
960 modify antagonistic interactions between commensal oral Streptococci
961 and *Streptococcus mutans*. Appl Environ Microbiol 85:e00370-19.
962 43. Svensäter G, Borgström M, Bowden GH, Edwardsson S. 2003. The acid-
963 tolerant microbiota associated with plaque from initial caries and healthy
964 tooth surfaces. Caries Res 37:395-403.
965 44. Marsh PD, Mcdermid AS, Keevil CW, Ellwood DC. 1985. Environmental
966 regulation of carbohydrate metabolism by *Streptococcus sanguis* NCTC
967 7865 grown in a chemostat. Microbiology 131:2505-2514.
968 45. Zeng L, Martino NC, Burne RA. 2012. Two gene clusters coordinate
969 galactose and lactose metabolism in *Streptococcus gordonii*. Appl Environ
970 Microbiol 78:5597-605.
971 46. Ramírez-Nuñez J, Romero-Medrano R, Nevárez-Moorillón GV, Gutiérrez-
972 Méndez N. 2011. Effect of pH and salt gradient on the autolysis of
973 *Lactococcus lactis* strains. Braz J Microbiol 42:1495-9.

974 47. Vilhena C, Kaganovitch E, Grünberger A, Motz M, Forné I, Kohlheyer D,
975 Jung K. 2019. Importance of pyruvate sensing and transport for the
976 resuscitation of viable but nonculturable *Escherichia coli* K-12. J Bacteriol
977 201.
978 48. Wu J, Li Y, Cai Z, Jin Y. 2014. Pyruvate-associated acid resistance in
979 bacteria. Appl Environ Microbiol 80:4108-13.
980 49. Ahn SJ, Hull W, Desai S, Rice KC, Culp D. 2020. Understanding LrgAB
981 regulation of *Streptococcus mutans* metabolism. Front Microbiol 11:2119.
982 50. Pfeiffer T, Morley A. 2014. An evolutionary perspective on the Crabtree
983 effect. Front Mol Biosci 1:17.
984 51. Deutscher J. 2008. The mechanisms of carbon catabolite repression in
985 bacteria. Curr Opin Microbiol 11:87-93.
986 52. Fleming E, Lazinski DW, Camilli A. 2015. Carbon catabolite repression by
987 seryl phosphorylated HPr is essential to *Streptococcus pneumoniae* in
988 carbohydrate-rich environments. Mol Microbiol 97:360-80.
989 53. Tong H, Zeng L, Burne RA. 2011. The EIIAB^{Man} PTS permease regulates
990 carbohydrate catabolite repression in *Streptococcus gordonii*. Appl
991 Environ Microbiol 77:1957-65.
992 54. Zeng L, Burne RA. 2010. Seryl-phosphorylated HPr regulates CcpA-
993 independent carbon catabolite repression in conjunction with PTS
994 permeases in *Streptococcus mutans*. Mol Microbiol 75:1145-1158.

995 55. Ge X, Shi X, Shi L, Liu J, Stone V, Kong F, Kitten T, Xu P. 2016.
996 Involvement of NADH oxidase in biofilm formation in *Streptococcus*
997 *sanguinis*. PLoS One 11:e0151142.
998 56. Baker JL, Derr AM, Faustoferri RC, Quivey RG, Jr. 2015. Loss of NADH
999 oxidase activity in *Streptococcus mutans* leads to Rex-mediated
1000 overcompensation in NAD+ regeneration by lactate dehydrogenase. J
1001 Bacteriol 197:3645-57.
1002 57. Takahashi N, Washio J, Mayanagi G. 2010. Metabolomics of
1003 supragingival plaque and oral bacteria. J Dent Res 89:1383-8.
1004 58. Gawron K, Wojtowicz W, Lazarz-Bartyzel K, Lamasz A, Qasem B, Mydel
1005 P, Chomyszyn-Gajewska M, Potempa J, Mlynarz P. 2019. Metabolomic
1006 status of the oral cavity in chronic periodontitis. In Vivo 33:1165-1174.
1007 59. Busuioc M, Buttaro BA, Piggot PJ. 2010. The *pdh* operon is expressed in
1008 a subpopulation of stationary-phase bacteria and is important for survival
1009 of sugar-starved *Streptococcus mutans*. J Bacteriol 192:4395-402.
1010 60. Korithoski B, Lévesque CM, Cvitkovitch DG. 2008. The involvement of the
1011 pyruvate dehydrogenase E1alpha subunit, in *Streptococcus mutans* acid
1012 tolerance. FEMS Microbiol Lett 289:13-9.
1013 61. Terleckyj B, Willett NP, Shockman GD. 1975. Growth of several cariogenic
1014 strains of oral streptococci in a chemically defined medium. Infect Immun
1015 11:649-55.

1016 62. Simpson JT, Wong K, Jackman SD, Schein JE, Jones SJ, Birol I. 2009.
1017 ABySS: a parallel assembler for short read sequence data. Genome Res
1018 19:1117-23.
1019 63. Lau PC, Sung CK, Lee JH, Morrison DA, Cvitkovitch DG. 2002. PCR
1020 ligation mutagenesis in transformable streptococci: application and
1021 efficiency. J Microbiol Methods 49:193-205.
1022 64. Rodriguez AM, Callahan JE, Fawcett P, Ge X, Xu P, Kitten T. 2011.
1023 Physiological and molecular characterization of genetic competence in
1024 *Streptococcus sanguinis*. Mol Oral Microbiol 26:99-116.
1025 65. LeBlanc DJ, Crow VL, Lee LN, Garon CF. 1979. Influence of the lactose
1026 plasmid on the metabolism of galactose by *Streptococcus lactis*. J
1027 Bacteriol 137:878-84.
1028 66. Moye ZD, Zeng L, Burne RA. 2014. Modification of gene expression and
1029 virulence traits in *Streptococcus mutans* in response to carbohydrate
1030 availability. Appl Environ Microbiol 80:972-985.
1031 67. Vujanac M, Iyer VS, Sengupta M, Ajdic D. 2015. Regulation of
1032 *Streptococcus mutans* PTS^{Bio} by the transcriptional repressor NigR. Mol
1033 Oral Microbiol 30:280-294.
1034 68. Schmittgen TD, Livak KJ. 2008. Analyzing real-time PCR data by the
1035 comparative C_T method. Nat Protocols 3:1101-8.
1036 69. Chen L, Walker AR, Burne RA, Zeng L. 2020. Amino sugars reshape
1037 interactions between *Streptococcus mutans* and *Streptococcus gordonii*.
1038 Appl Environ Microbiol 87:e01459-20.

Figure legends

Figure 1. A *manL* mutant of *S. sanguinis* SK36 had enhanced viability in stationary cultures. Wild-type strain SK36 (MMZ1612), the *manL* mutant, and the complemented derivative of *manL* (*manLComp*) were (n = 3) cultivated for 20 h in BHI before being diluted into fresh BHI (A) or a TY medium containing 20 mM of glucose (TYG20) (B), followed by growth monitoring in a Bioscreen system. For another set of SK36 samples (SK36 + Kp), 50 mM of potassium phosphate buffer (pH 7.2) was added to the overnight cultures. (C) An *in vitro* sugar phosphorylation assay was carried out using SK36 and *manL* mutant cultures prepared with BHI medium and harvested at the exponential phase. (D) For measurements of lactate, overnight cultures were diluted into TY containing glucose (Glc) or lactose (Lac), and the supernates were harvested at the exponential phase. The results are the averages of three biological replicates with error bars denoting standard deviations. Asterisks represent statistical significance according to a Student's *t* test (*, P <0.05; **, P <0.01, ***, P <0.001).

Figure 2. pH drop assays. Strains SK36 (MMZ1612), *manL,* and *manLComp* were cultured to late exponential phase (OD_{600} = 0.8) in 50 mL BHI medium, harvested by centrifugation and used immediately for assay (A) or frozen at -80°C, and then thawed and assayed at least one day later (B). Each sample was washed once with 50 mL cold water, resuspended in a solution containing 50 mL KCl and 1 mM $MgCl_2$, and normalized to OD_{600} = 4.5. The assay was initiated by the addition of 50 mM glucose and pH was monitored and recorded at 30-s

1062 intervals for at least 40 min. Each curve includes the average and standard
1063 deviation (error bars) of three biological replicates.
1064
1065 **Figure 3.** Loss of *manL* affects pH homeostasis by changing AD gene
1066 expression. pH measurements of stationary-phase cultures (20 h) in TY (A, B) or
1067 BHI (C) media were recorded for strains SK36 (MMZ1612), *manL, manLComp*,
1068 *arcA* and *manL arcA.* For BHI cultures, 0, 1, or 5 mM of arginine was added to
1069 the medium before cultivation. Data were obtained from three biological
1070 replicates. (D) RT-qPCR was performed to measure the expression of *arcA* gene
1071 in exponential-phase cultures prepared in TY containing glucose (Glc) or lactose
1072 (Lac), or in BHI. The abundance of *arcA* mRNA was calculated relative to an
1073 internal control (*gyrA*). Three biological replicates were included for each sample
1074 and the results are their averages and standard deviations (as error bars).
1075
1076 **Figure 4.** H_2O_2 production (A) and antagonism of *S. mutans* (B) on plates.
1077 Cultures of SK36 the wild type (strain #1) and its mutant derivatives deficient in
1078 *manL* (#2), *ccpA* (#3), *manL ccpA* (#4), *nox* (#5), and *manL nox* (#6) were each
1079 dropped onto the surface of TY-agar plates prepared with 20 mM of glucose,
1080 lactose, galactose (Gal), GlcN, GlcNAc, or 10 mM each of glucose and galactose
1081 (Glc/Gal), and incubated for 24 h in an aerobic environment (with 5% CO_2). (A)
1082 For direct measurement of H_2O_2 release, the plates contained 0.1% each of
1083 $FeCl_3.6H_2O$ and potassium hexacyanoferrate(III) which formed a Prussian blue
1084 zone upon reacting with H_2O_2. (B) For antagonism of *S. mutans*, same amount of

1085 UA159 culture (*S. m*) was placed to the right of the first colony, followed by
1086 another 24 h of incubation. All images were photographed under the same
1087 setting, with the zones of Prussian blue assessed relative to the size of the
1088 colonies. Each experiment was repeated three times using biological replicates,
1089 with a representative result being presented.
1090
1091 **Figure 5.** Measurements of relative mRNA levels of catabolic genes by RT-
1092 qPCR. Strains SK36, *ccpA*, *manL*, and *manL ccpA* were each cultured, in a TY
1093 medium containing 20 mM glucose, to exponential phase before harvested for
1094 RNA extraction. An internal control (*gyrA*) was used to measure the relative
1095 abundance of each transcript. The results for each gene are presented as the
1096 average and standard derivation (error bar) of three biological repeats.
1097
1098 **Figure 6.** Deletion of *manL* affects release of pyruvate (A, B, C) and eDNA (D).
1099 Strains SK36, *manL*, *manLComp*, *ccpA*, and *manL ccpA* were cultured in TY
1100 medium supplemented with 20 mM of glucose (A, B, C, D) or 10 mM of lactose
1101 (A). (A) Supernates from stationary-phase (20 h) cultures of all 5 strains were
1102 used in an LDH-catalyzed reaction to measure the pyruvate levels under glucose
1103 and lactose conditions. Aliquots of SK36 (B) or the *manL* mutant (C) were taken
1104 at specified time points for measurements of OD_{600} and extracellular pyruvate.
1105 (D) Supernates from stationary cultures of SK36, *manL*, and *manLComp* were
1106 measured for DNA concentrations using a fluorescent dye. The relative
1107 fluorescence units (RFU) are in linear relationship with DNA concentrations

within the experimental range. Each result shows the average of three biological repeats, with the error bars denoting standard derivation and asterisks the statistical significance according to Student's *t* test (**, *P* <0.01; ***, *P* <0.001).

Figure 7. Exogenous pyruvate improves persistence of *S. sanguinis*. *S. mutans* UA159 and *S. sanguinis* strains SK36 and its isogenic *manL* mutant were each (n = 3) cultured overnight in BHI medium supplemented with or without 5 mM of pyruvate. The next day, cultures were diluted and plated for viable CFU counts (A) or for assessment of growth characteristics (B, C) by diluting into TY-Glc medium with or without 5 mM of pyruvate. Panel B shows the effects of pyruvate in overnight cultures of UA159 and SK36 by diluting them into TY-Glc without pyruvate, and panel C shows the effects of pyruvate added to fresh TY-Glc by diluting from overnight cultures prepared without pyruvate. Each of the columns and the growth curves represents the average of three biological replicates. Asterisks denote the statistical significance (*P* <0.05) obtained using a Student's *t* test.

1125 **Table 1.** Bacterial strains used in this study.

Strains	Relevant characteristics[a]	Source or reference
MMZ1612	*S. sanguinis* SK36 stock 1	Lemos laboratory
MMZ1896	*S. sanguinis* SK36 stock 2	Kitten laboratory
MMZ1922	*S. sanguinis* SK36 stock 3	ATCC BAA-1455
MMZ1616	SK36 *manL::Em*	MMZ1612
MMZ1617	SK36 *manL::Km*	MMZ1612
MMZ1882	SK36 *manL::Km*	MMZ1896
MMZ1923	SK36 *manL::Km*	MMZ1922
MMZ1904	SK36 *manLComp*::*Km*	MMZ1616
MMZ1905	SK36 *manLComp*::*Em*	MMZ1617
MMZ1911	SK36 *arcA::Km*	MMZ1896
MMZ1912	SK36 *arcA::Em manL::Km*	MMZ1617
MMZ1913	SK36 *ccpA::Km*	MMZ1896
MMZ1910	SK36 *ccpA::Em manL::Km*	MMZ1617
MMZ1906	SK36 *nox::Km*	MMZ1896
MMZ1907	SK36 *nox::Em manL::Km*	MMZ1617
UA159	*S. mutans* wild type, *perR*$^+$	ATCC 700610

1126 [a] *Km* indicates kanamycin resistance; *Em*, erythromycin.

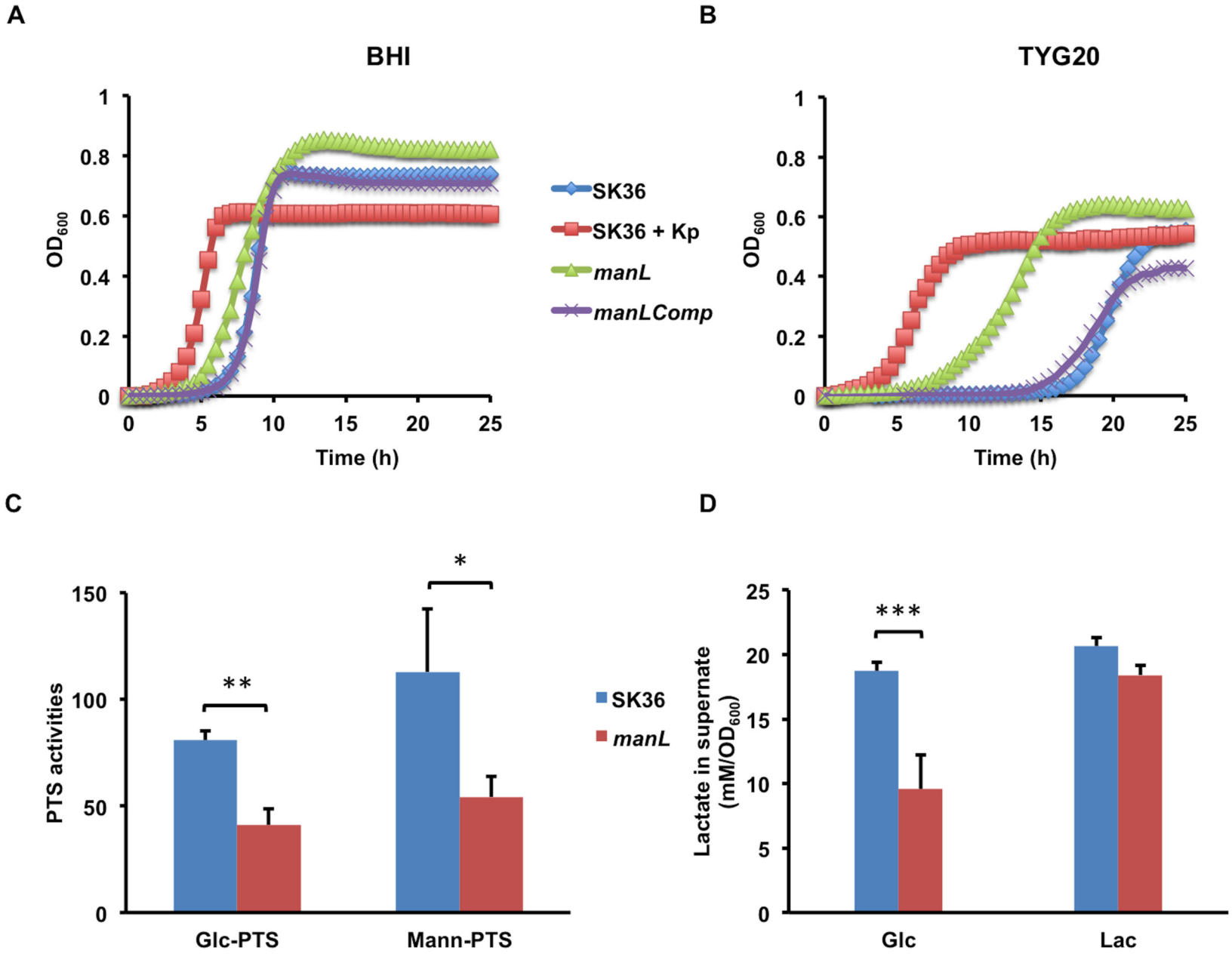

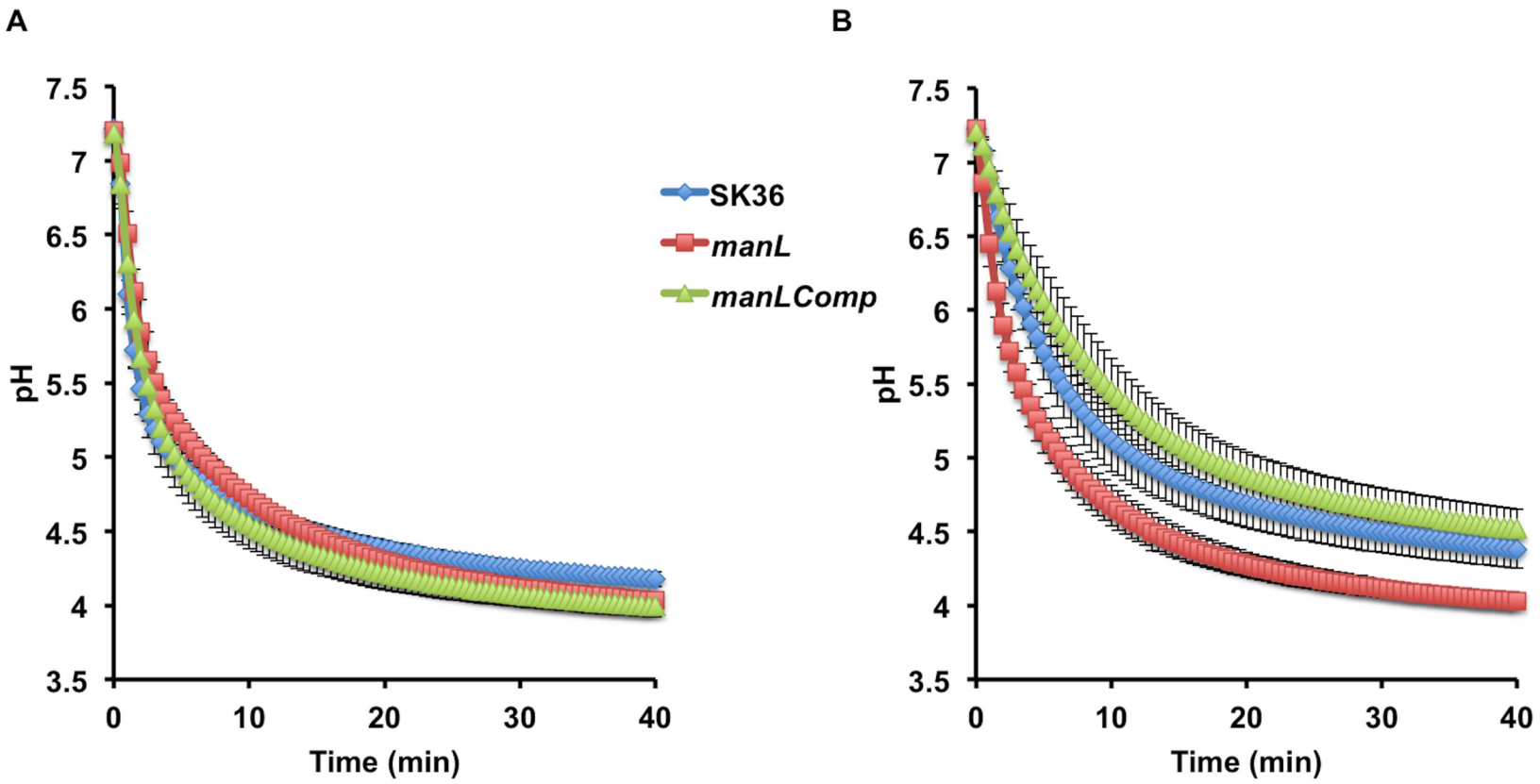

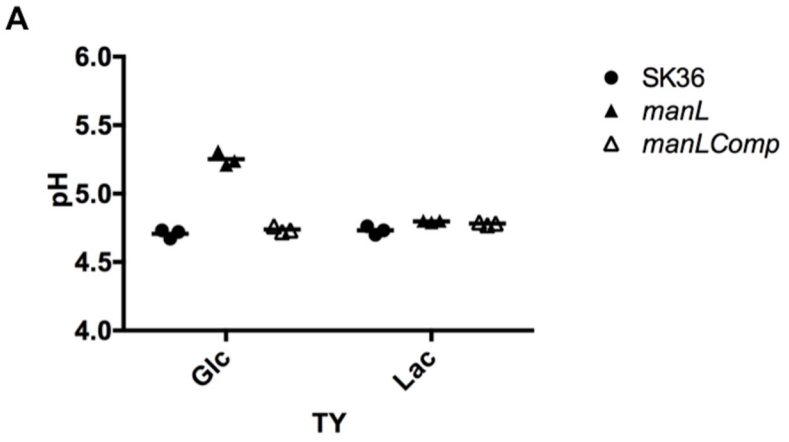

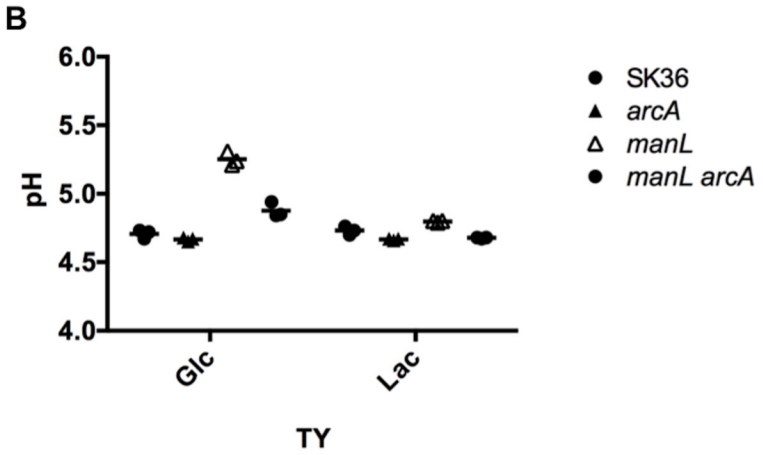

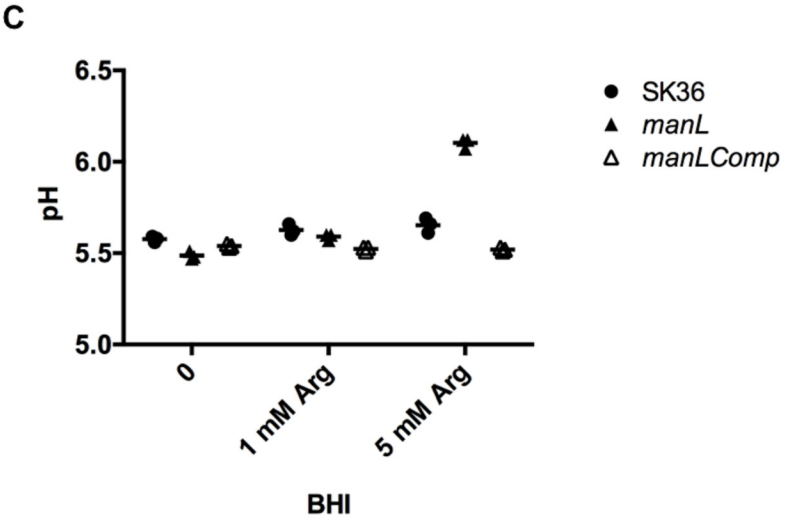

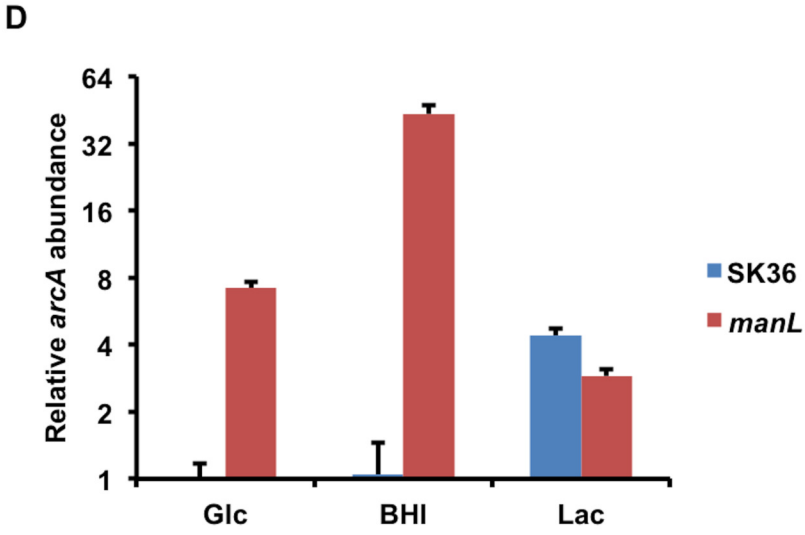

A

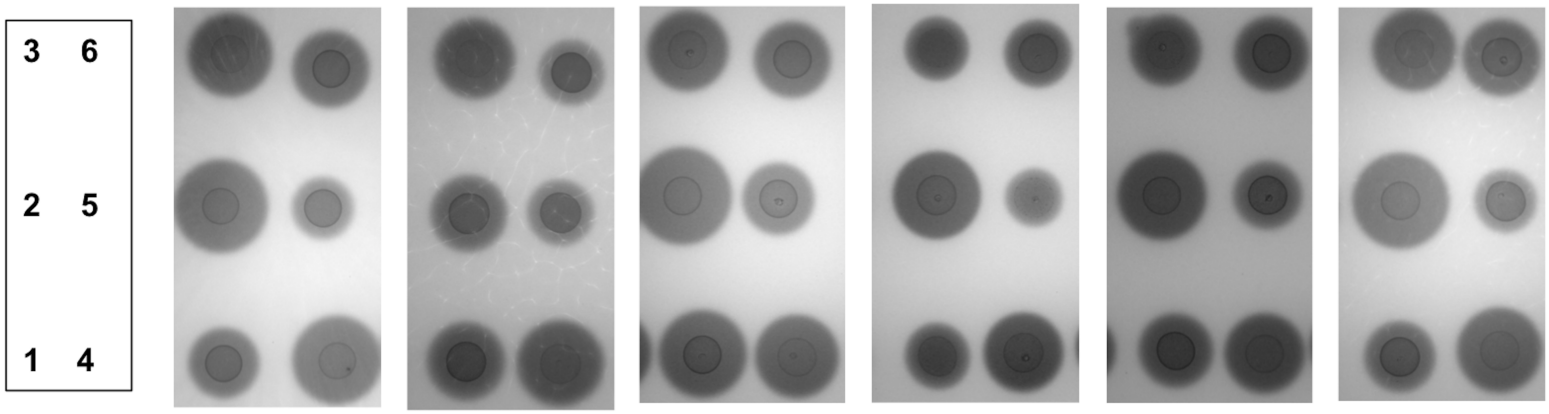

B